State-selective capture in collisions between ions and ground- and excited-state alkali-metal atoms

J. Pascale
Service de Physique des Atomes et des Surfaces, Centre d'Etudes Nucléaires de Saclay, 91191 Gif-sur-Yvette CEDEX, France

R. E. Olson and C. O. Reinhold
Department of Physics, University of Missouri–Rolla, Rolla, Missouri 65401
(Received 21 May 1990)

Total cross sections for state-selective electron capture in collisions between ions and alkali-metal atoms have been calculated by means of a three-body classical-trajectory Monte Carlo (CTMC) method using model potentials to describe the electron–ionic-core interactions. Calculations have been performed for Na^+-Na($28d$) collisions and for N^{5+} and Ar^{8+}-Cs($6s$) collisions. The collision velocity range corresponds to $0.5 \lesssim v_p/v_e \lesssim 2$, where v_p is the projectile velocity in the laboratory frame and v_e is the initial orbital velocity of the electron bound to the alkali-metal core. In the case of $Na^+ + Na(28d)$ collisions, calculations of the final n,l,m distributions show the importance of the electron-capture cross sections into states with $m > 1$. For the case of multiply charged ion—Cs($6s$) collisions, a predominance of electron capture to nearly circular states (large l values) is predicted for cross sections near the maximum of the n distribution. When the e^--Cs^+ interaction is described by a realistic model potential, the CTMC calculations are found to be in good agreement with recent measurements of the final n values that are predominantly populated after single-electron capture.

I. INTRODUCTION

Recent interest in multiply-charged-ion collisions with neutral atoms has been motivated not only by their importance in plasma physics and thermonuclear fusion, but also for reasons of fundamental research. In particular, at low to intermediate energies, electron capture occurs with high efficiency because of the strong Coulomb interaction between the projectile and the target electron. For these collisions, it is well known that the electron is captured by a multiply charged projectile to highly excited levels.[1]

When the target is initially in a high Rydberg state, the efficiency of one-electron capture, which scales approximately as n_i^4 (see, for example, Ref. 2), may be so large that one could produce doubly excited Rydberg states in an experiment where two electrons would be captured in two successive collisions of the multiply charged projectile with the Rydberg atom targets.[3] In such an experiment, it is very important to know the n,l,m distributions of the captured electron after the first collision.

The theoretical approach to these problems by means of quantum-mechanical or semiclassical methods is intractable in view of the large number of channels that are coupled, which must include the ionization and excitation channels in order to accurately compute the electron-capture cross sections in the intermediate energy range. Because of the strength of the Coulomb interactions, perturbative methods are also inappropriate to describe these collisions. An alternative approach is to use the three-body classical-trajectory Monte Carlo (CTMC) method[1,4,5] which was first proposed by Abrines and Percival[6] for H^+-H($1s$) collisions. Although most of the applications of this method have used pure Coulomb interactions, a generalization to make use of more realistic effective interactions between the valence electron and the ionic cores has successfully been developed recently.[7–9]

One purpose of the present work is to assess the validity of the CTMC method by comparison with two sets of experimental data concerning the final n-level distributions of the captured electron in two types of ion-atom collisions: namely, the collision of a singly charged ion with a Rydberg atom, and the collision of a highly charged ion with a ground-state atom. In both cases the electron is captured to highly excited states and, therefore, this process is expected to be well described by a classical model. However, the two types of collisions differ markedly in the initial state of the target and the cross sections could be sensitive to the choice of interaction between the electron and the target core. Thus, the CTMC method is tested here with two different types of e^--core interactions: a pure Coulomb and a more realistic model potential.

Recently, there have been extensive experimental studies of the electron-capture process for collisions of singly charged ions X^+ (with X=Ne, Ar, and Na) with Na targets in excited Rydberg states $n_i \simeq 24-34$, $l_i = 0,2$.[10–12] The collision velocity range explored in these works was $0.6 \lesssim v_p/v_e \lesssim 2.0$, where v_p is the velocity of the impinging ion in the laboratory frame and v_e is the initial orbital velocity of the valence electron. A field-ionization detection technique was used to determine the final n-level distributions of the captured electron. The measurements

were analyzed in terms of adiabatic field-ionization processes which assume a preferential population of final states with $m=0,1$ (the projection of the final angular momentum of the Rydberg electron onto the incident beam direction).

CTMC calculations for collisions involving initial n,l Rydberg states were carried out previously by Becker and MacKellar[5] who used Coulomb interactions between the valence electron and the ionic cores. In the case of the $Na^+ + Na(28d)$ collisions, these authors found, for $v_p/v_e = 1.658$, good agreement between the calculated and the relative measurements[12] of the final n-level distribution for both the shape and the position of the peak of the distribution. However, for $v_p/v_e = 1.0$, they found that the position of the theoretical peak of the n-level distribution was shifted to larger n values in comparison with the experimental findings of Rolfes and MacAdam[12] by $\Delta n \simeq 6$. The reason for this discrepancy was not clear and, in an attempt to explain it, MacKellar and Becker[13] mentioned preliminary calculations of final m distributions which were found to be broadly peaked around $m=0$. Because of the small number of trajectories used in their calculations (less than 18 000), no definitive conclusion was drawn by these authors about the discrepancy, making doubtful the validity of the CTMC calculations for $v_p/v_e \lesssim 1.0$, and also very intriguing the apparent good agreement between CTMC calculations and experimental data for $v_p/v_e = 1.658$. Indeed, MacAdam and colleagues[14,15] have recently concluded that the interpretation of the experimental measurements should be revised to account for diabatic field ionization after capture to $m > 1$ states. It is therefore important to perform large scale CTMC calculations (up to 10^6 trajectories) which yield final n,l,m distributions with small statistical errors for both values of v_p/v_e. These CTMC results may then be useful to guide the analysis of the experimental data.

More recently, Martin *et al.*[16] have reported optical spectroscopic studies of the electron-capture process in N^{5+} and Ar^{8+}-Cs(6s) collisions at an impact energy of 80 keV (corresponding to $v_p/v_e = 0.89$ and 0.53, respectively). These studies were able to determine unambiguously the predominant final n-state population after single-electron capture (note that the valence electron is captured to highly excited levels since the projectile is a multiply charged ion). It is important to compare the CTMC results with these measurements since the experimental technique used for the detection of the final n-levels is completely different from the one used by MacAdam and co-workers.[10–12,14,15] Also, it is useful to test the CTMC method in these cases since the range of collision velocities corresponds to $v_p/v_e \lesssim 1$ and core effects are expected to be significant for the description of the initial state of the Cs target.

II. THEORETICAL APPROACH

In the present calculations we use the CTMC method as described previously in detail by Reinhold and Falcón.[9] The CTMC method is based on solving the Hamilton's equations of motion for the three-body system (the valence electron, the alkali-metal core, and the ionic core projectile), given a set of initial conditions for the projectile and the target. As in the method of Abrines and Percival,[6] once the electronic energy of the target atom is specified, the initial classical orbit of the valence electron about the core target is determined by five parameters that are randomly selected from a microcanonical distribution. However, the method of Reinhold and Falcón[9] differs from other methods in that two successive changes in the variables allow one to avoid the integration of the Kepler's equations. In addition, the initial orbital quantum number l_i of the target is specified by the classical angular momentum $\mathbf{l}_c = \mathbf{r}_i \times \mathbf{k}_i$ and the condition

$$l_i \leq l_c < l_i + 1 , \tag{1}$$

where $\mathbf{r}_i$ and $\mathbf{k}_i$ are, respectively, the position and momentum vectors of the valence electron relative to the core target.

The initial conditions for the projectile are specified by its position relative to the target, its velocity v_p and the impact parameter b which is determined from a random selection of b^2 in the interval $[0, b_{\max}^2]$ where $b_{\max}$ is the maximum impact parameter that contributes significantly to the capture or ionization processes. The initial velocity of the projectile is along the z axis.

The general form of the model potential employed to describe the interaction between the valence electron and the projectile or target ionic core is

$$V(r) = -\frac{1}{r}[Z + N(1 + ar + br^2)\exp(-cr)] - \tfrac{1}{2}\alpha_d \frac{r^2}{(r^3 + r_c^3)^2} - \tfrac{1}{2}\alpha_q' \frac{r^3}{(r^3 + r_c^3)^3} , \tag{2}$$

where Z and N are the charge and number of electrons of the ionic core; α_d is the dipole polarizability of the core; $\alpha_q' = \alpha_q - 6\beta$ with α_q the quadrupole polarizability of the core and β is a dynamical correction; r_c is a cutoff radius. The parameters a, b, c, and r_c are chosen to fit the spectroscopic data,[17] and for the ionic cores considered in this paper they are given in Table I along with the other constants.

Even though total cross sections for both ionization and electron capture were calculated, only electron-capture cross sections are reported in this work. The final substate distributions were obtained in the following manner. In the cases that we have considered, because the valence electron is captured by the projectile to a highly excited state with a preferential population of large l, we can safely ignore the quantum defect of the final state. Thus, we define a classical number n_c related to the calculated binding energy E_p of the electron relative to the ionic core projectile as

$$E_p = -\frac{Z_p^2}{2n_c^2} , \tag{3}$$

where Z_p is the charge of the projectile ionic core. Then we relate n_c to the quantum number n of the final state by the condition[5]

TABLE I. Parameters for the electron-ionic core model potential [see Eq. (2)]. The dipole and quadrupole polarization α_d and α'_q, and the cutoff radius r_c are in atomic units.

Ionic core	Z	N	a	b	c	α_d	α'_q	r_c
Na^+	1	10	−0.3154	0.2082	2.34	0.9457	−0.609	0.798
Cs^+	1	54	−1.956	1.918	2.28	16.3	−22.8	1.989
N^{5+}	5	2	−0.4078	0.1888	6.0	0	0	
Ar^{8+}	8	10	−1.706	1.039	3.5	0	0	

$$[(n-\tfrac{1}{2})(n-1)n]^{1/3} \leq n_c < [n(n+\tfrac{1}{2})(n+1)]^{1/3} . \quad (4)$$

From the normalized classical angular momentum $l_c = (n/n_c)(\mathbf{r}\times\mathbf{k})$, where now $\mathbf{r}$ and $\mathbf{k}$ are referred to the projectile ionic core, we relate l_c to the orbital quantum number l of the final state as

$$l \leq l_c < l+1 \quad (5)$$

and, in the same manner, we define the absolute value m (magnetic quantum number) of the final state from $m_c = |l_c^z|$ as

$$m \leq m_c < m+1 . \quad (6)$$

In principle, it is also possible to analyze the final-state distributions from the effective quantum number

$$n^* = n - \delta_l \quad (7)$$

where δ_l is the quantum defect. In that case we would have to consider at the same time conditions (4) and (5) with n replaced by n^*, and then the value n of the final state is obtained from Eq. (7). However, in this work we have found that large values of l are preferentially populated in the electron-capture process, so there was no need to employ Eq. (7).

The domain of validity of the classical-trajectory method is difficult to assess and its definition mainly rests by comparisons with experimental or quantum-mechanical calculations when available. From such comparisons in $H^+ + H(1s)$ collisions, it is now generally assumed that the CTMC method is valid in the range

$$1 \lesssim v_p/v_e \lesssim 4 . \quad (8)$$

This range of validity is found to become wider when the electron is captured to excited Rydberg states, which occurs, for example, when the projectile charge is greater than the target charge or when the target is initially in an excited state.

III. RESULTS AND DISCUSSION

A. $Na^+ + Na(28d)$ collisions

The calculated total cross sections for the electron capture in $Na^+ + Na(28d)$ collisions at $v_p/v_e = 1.0$ and 1.658 are shown in Figs. 1(a) and 1(b) as a function of the n-quantum number of the captured electron. The cross sections displayed in the figures were obtained with the effective interaction given in Eq. (2). We have verified that calculations performed with pure Coulomb interac-

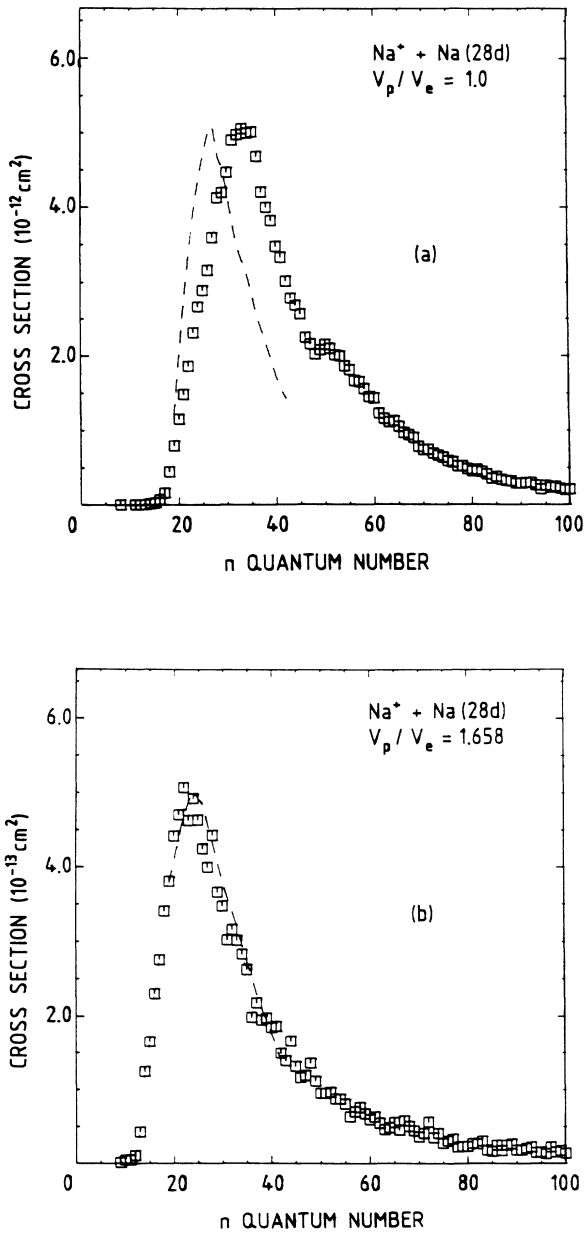

FIG. 1. The electron-capture n distribution for $Na^+ + Na(28d)$ collisions at (a) $v_p/v_e = 1.0$ and (b) $v_p/v_e = 1.658$. The present theoretical results (open squares) are compared to the relative experimental data of Rolfes and MacAdam (Ref. 12) (dashed line), which were normalized at the peak of the n distribution.

tions show no significant changes and agree with the previous CTMC calculations of Becker and MacKellar[5] within 35%. Also shown in Figs. 1(a) and 1(b) are the relative (not absolute) experimental data of Rolfes and MacAdam[12] normalized to the magnitude of our maximum. The experimental values were reported assuming the final Stark number equal to the final n. As already observed by Becker and MacKellar,[5] the agreement between the calculated n distribution and the experimental one is quite good for $v_p/v_e=1.658$. For $v_p/v_e=1.0$, the calculated n-distribution peaks at about $n=33$, in variance with the experimental data which peaks at $n\simeq 27$. Also, the calculated width of the n-distribution at half maximum is $\Delta n\simeq 20$ compared with the experimental result $\Delta n\simeq 15$.

In order to understand the origin of the discrepancy between experiment and theory for $v_p/v_e=1.0$ and the apparent agreement for $v_p/v_e=1.658$, it is useful to evaluate for both cases the population of final states with different m values of the captured electrons, since this distribution plays a very important role in the experimental analysis of field ionization of specific n levels. Indeed, if there is a significant population of $m>1$ sublevels, the final states could field ionize via diabatic transitions. Rolfes and MacAdam[12] originally estimated that this population could cause an error in the position of the experimental peak in the n distribution of at least $\Delta n\simeq -4$. However, on the basis of predictions by the Brinkman-Kramers approximation, these authors discarded this possibility and assumed adiabatic ionization ($m\leq 1$).

Figure 2 shows the calculated n,m distribution for $n=33$ corresponding to the peak, in the case of $v_p/v_e=1.0$. The cross sections which are reported in the figure are defined as

$$\sigma(n=33,m)=\sum_l \sigma(n=33,l,m)\ . \tag{9}$$

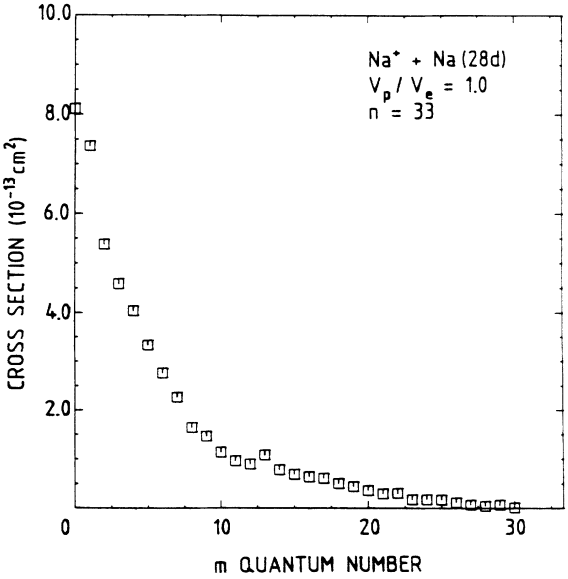

FIG. 2. The calculated n,m distribution [Eq. (9)] for electron capture into $n=33$ in $Na^+ + Na(28d)$ collisions at $v_p/v_e=1.0$.

The calculated n,m distribution is peaked at $m=0$, is relatively wide, and has a half-width of $\Delta m\simeq 5$. Interestingly, final states with $m\geq 2$ contribute more than 60% to the total capture cross section $\sigma(n=33)$. Similar n,m distributions are also obtained for different final n values, and also in the case of $v_p/v_e=1.658$. Further, we have obtained similar results for different n_i,l_i initial states.

Therefore, we conclude that diabatic processes cannot be neglected in the experimental determination of the final n distribution by means of a field-ionization technique. This holds not only for $v_p/v_e\leq 1$, but also for $v_p/v_e>1$. This conclusion has also been obtained very recently by MacAdam *et al.*[14,15] who have verified that captured electrons may ionize in the detector primarily by diabatic rather than via adiabatic field ionization as formerly assumed. More specifically, because a wide distribution of m-final states is created during the electron-capture process, an observed ionization peak may correspond to many n-final states which field ionize adiabatically or diabatically and contribute differently to the ionization peak. Thus, the experimental determination of the final n-level distribution by means of a field-ionization technique becomes very intricate not only for $v_p/v_e\leq 1$ but also for $v_p/v_e>1$. Largely for this reason, it is difficult to understand the apparent good agreement that has been generally observed between the experimental and calculated positions of the peaks in the n distributions for $v_p/v_e>1$. A more direct comparison between experiment and theory would be to apply the field-ionization technique under the experimental conditions to the theoretical n,l,m distributions and compare then the theoretical ion signal to the experimental one. In any case, it is clear from our results that some theoretical guidance has to be provided for the analysis of the experimental data. In this respect, the present results may be quite useful.

The percentages of final m and l values obtained for the total electron capture in $Na^+ + Na(28d)$ collisions are shown in Figs. 3(a) and 3(b) for $v_p/v_e=1.0$ and 1.658, respectively. Since these percentages are found to be similar for the two values of v_p/v_e considered here, we will mainly discuss the case $v_p/v_e=1.0$ [Fig 3(a)]. It may be seen that less than 28% of final $m=0,1$ values are created in the electron-capture reaction. The l distribution is found to be wide, peaked at about $l=16$, with a width at half maximum of about $\Delta l=17$. The large l values that are obtained may be explained by the large impact parameters which contribute mainly to the electron-capture process [see Figs. 4(a) and 4(b)]. However, it may be seen that for $l\gtrsim 25-30$ the populations are small. This appears to be related to the very large l mixing that takes place in the target during the collision.[18] On these grounds, and because the captured electron tends to preserve its binding energy and the size of its initial orbit,[1] final states with $l\lesssim n_i-1$ should be preferentially populated. Indeed, this is clearly seen in Figs. 5(a)–5(c), where the electron-capture n,l distribution,

$$\sigma(n,l)=\sum_m \sigma(n,l,m) \tag{10}$$

is reported versus l for $v_p/v_e=1.0$ and for typical final

values $n=33$, 24, and 45, corresponding to n values at the peak and half of the peak of the n distribution [see Fig. 1(a)]. The n,l distribution increases with l up to a broad maximum at $l \simeq 18-25$ and then decreases abruptly to take very small values for $l \gtrsim 28$ [see Fig. 5(a)]. When n decreases or increases with respect to $n \simeq 33$, the peak in the n,l distribution shifts towards smaller values. However, appreciable changes in the shape of the n,l distribution can be seen depending if n is smaller or greater than $n \simeq 33$. Specifically, for $n \lesssim 33$ the n,l distribution is wide and extends continuously from $l=0$ to the maximum allowed value $n-1$ [see Fig. 5(b)], whereas for $n \gtrsim 33$ the distribution presents a narrow peak and then decreases rapidly to take very small values for $l \gtrsim 25$ [see Fig. 5(c)].

The n,l,m distributions for the l values which correspond to the positions of the maxima of the l distributions of Figs. 5(a)–5(c) are displayed in Figs. 6(a)–6(c), respectively. For $n=33$ and 45 the n,l,m distributions are peaked at small m values. However, the n,l,m distribution for $n=45$, $l=18$ is found to be wider than the one for $n=33$, $l=21$. In contrast, the n,l,m distribution for $n=24$, $l=16$ is much broader. However, in this case the statistical uncertainties are quite large and preclude an accurate comparison to the other two cases.

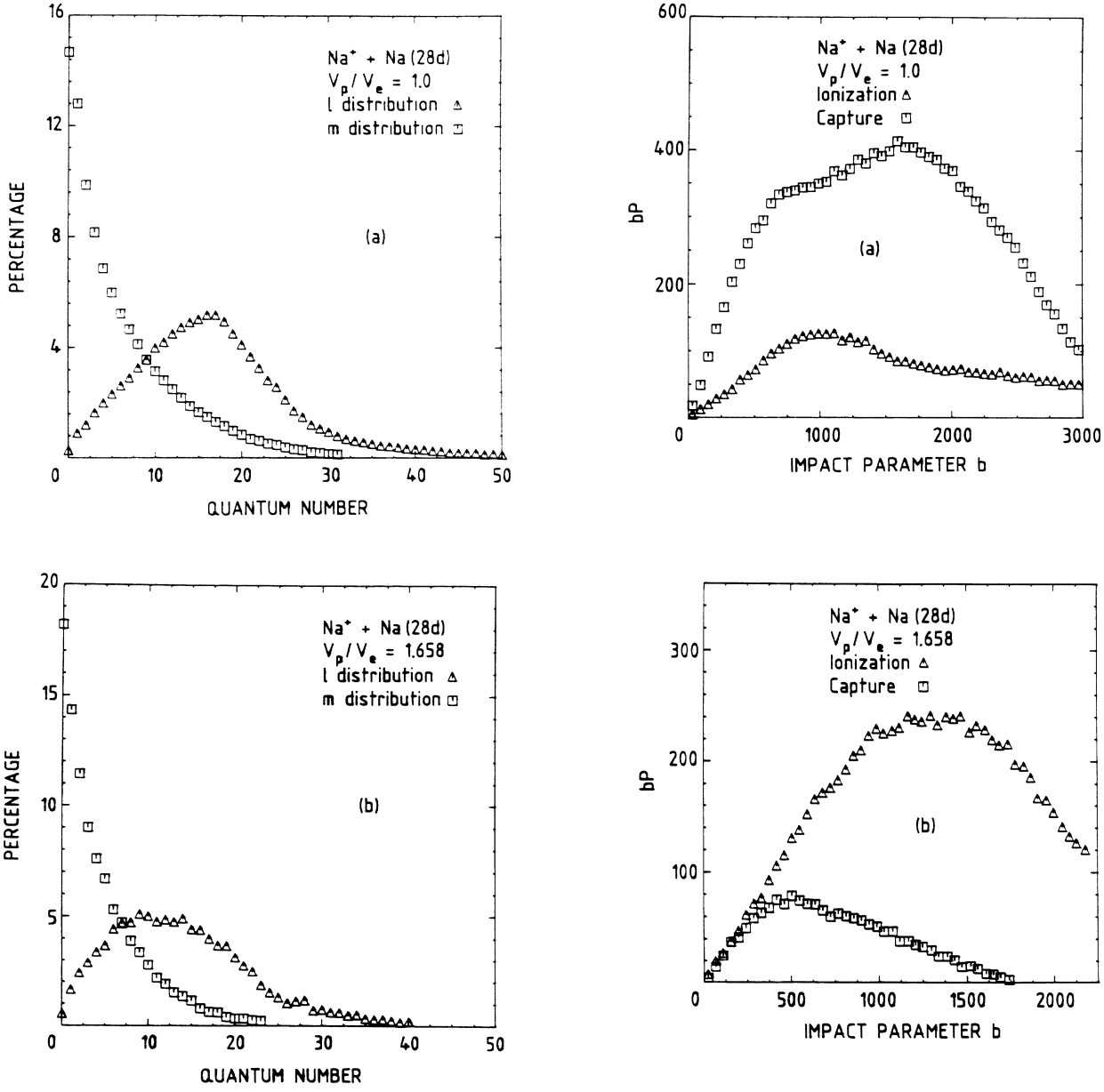

FIG. 3. The calculated percentages of final m and l values for electron capture in $Na^+ + Na(28d)$ collisions at (a) $v_p/v_e=1.0$ and (b) $v_p/v_e=1.658$.

FIG. 4. The calculated probability of electron capture (open squares) and ionization (open triangles) times the impact parameter in $Na^+ + Na(28d)$ collisions at (a) $v_p/v_e=1.0$ and (b) $v_p/v_e=1.658$.

B. N^{5+}, Ar^{8+} + Cs(6s) collisions

In Figs. 7(a) and 7(b) we compare the electron-capture n distributions that are obtained by using either Coulomb or effective interactions between the valence electron and the cores for N^{5+} + Cs(6s) and Ar^{8+} + Cs(6s) collisions at impact velocities $v_p/v_e = 0.894$ and 0.529, and taking into consideration 2×10^4 and 1.2×10^4 trajectories, respectively. Here, we have verified that projectile core effects are unimportant since large n and l values are preferentially populated. However, target core effects are seen to be quite significant for both the magnitude and the position of the peak of the n distribution. In the case of Coulomb interactions the peak is smaller and shifted toward smaller n values by about 1 when compared to the case of effective interactions. According to the recent experimental measurements of Martin *et al.*[16] for the same collision systems, the n values of the final states that are predominantly populated are found to be $n=7,8$ and $n=10,11$ for the cases of N^{5+} and Ar^{8+} projectiles, respectively. These experimental results, which were obtained unambiguously from the relative intensities of the observed lines, are found to be in good agreement with the CTMC calculations obtained by using a model potential to describe the e^--Cs^+ interaction.

The n,l distributions [Eq. (10)] corresponding to typi-

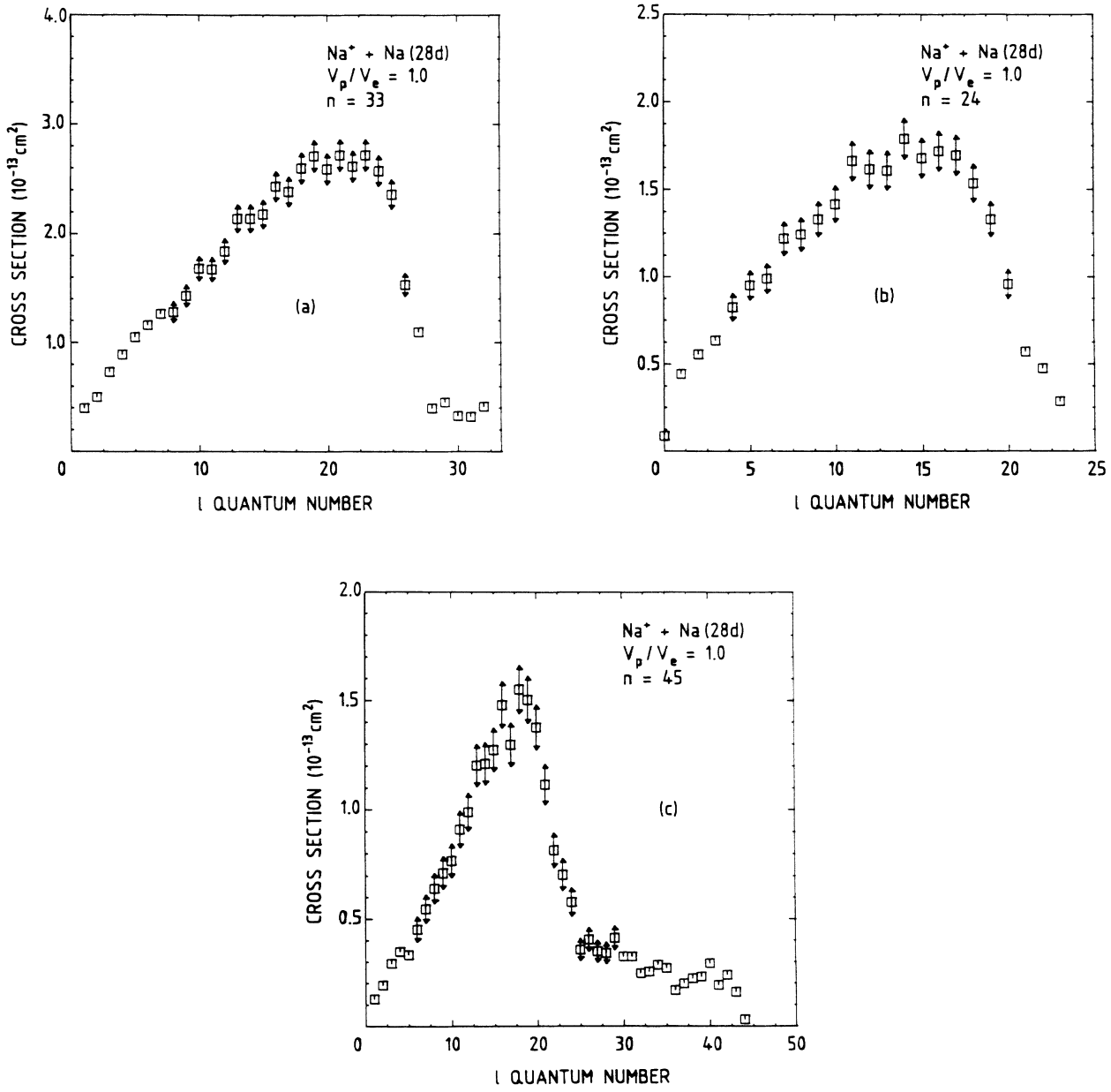

FIG. 5. The calculated n,l distribution [Eq. (10)] for electron capture in Na^+ + Na(28d) collisions at $v_p/v_e = 1.0$ for (a) $n=33$, (b) $n=24$, and (c) $n=45$.

cal n values are displayed in Figs. 8(a) and 8(b) for the $N^{5+}+Cs(6s)$ and $Ar^{8+}+Cs(6s)$ collisions, respectively. In these calculations and the following, we have utilized the effective potential of Eq. (2) to describe the e^--Cs^+ interaction. The n,l distributions are found to behave quite similarly for both collision systems. In general, it is seen that the largest possible values of l are preferentially populated in the electron-capture process. Interestingly, the rate of increase of the cross sections with l is found to be very different depending on the value of n. In fact, the n,l distribution is very sharply peaked for n values near the maximum of the n distribution [see $n=7,8$ in Fig. 8(a) and $n=10,11$ in Fig. 8(b)], whereas it becomes more statistical for n values far from the maximum. Once again, the population of large l values is closely related to the domains of impact parameters b that contribute to the total capture process in $N^{5+}+Cs(6s)$ and $Ar^{8+}+Cs(6s)$ collisions (see Fig. 9). That is, l is related to b in a very simple picture as $l \simeq m_e b v_p$, m_e being the electron mass. Finally, we note that for these collision systems and at the impact energies considered here, the ionization process is found to be negligible.

In Fig. 10 we display the n,l,m distributions for $n=7$, $l=6$ in $N^{5+}+Cs(6s)$ collisions as well as for $n=10$, $l=9$ in the case of $Ar^{8+}+Cs(6s)$ collisions. The n,l,m distribution for N^{5+} projectiles is found to be peaked at $m=0$

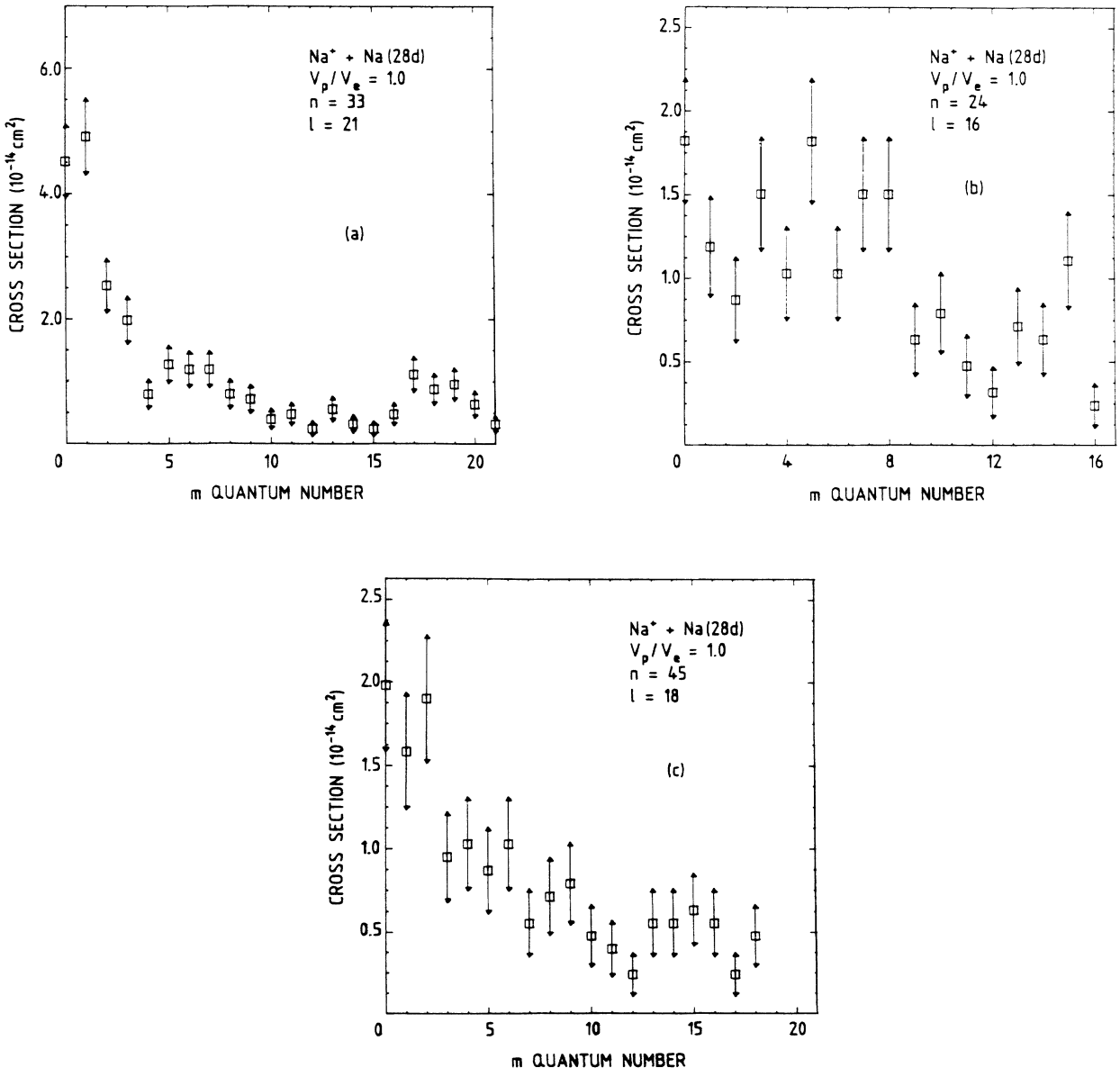

FIG. 6. The calculated n,l,m distribution for electron capture in $Na^+ + Na(28d)$ collisions at $v_p/v_e=1.0$ for (a) $n=33$, $l=21$, (b) $n=24$, $l=16$, and (c) $n=45$, $l=18$.

and then decreases monotonically for increasing m values. On the other hand, the n,l,m distribution for Ar^{8+} projectiles is found to be wider and to exhibit its maximum at $m=0,1$. This is due to the greater Coulomb field of Ar^{8+} which allows electrons to be captured to orbits that are not coplanar with the scattering plane.

Finally, in Fig. 11 we report the percentages of final m and l values obtained for the electron-capture process in $N^{5+}+Cs(6s)$ and $Ar^{8+}+Cs(6s)$ collisions. In contrast with the case of $Na^{+}+Na(28d)$ collisions, about 82% and 64% of the total capture cross section correspond to final $m=0,1$ values for N^{5+} and Ar^{8+} projectiles, respectively. Interestingly, this percentage decreases from N^{5+} to Ar^{8+}. This behavior is consistent with the results obtained for $Na^{+}+Na(28d)$ collisions, since more highly excited states are populated in $Ar^{8+}+Cs(6s)$ collisions than in $N^{5+}+Cs(6s)$ collisions. Accordingly, the l distributions peak at larger l values for Ar^{8+} projectiles than for N^{5+} projectiles.

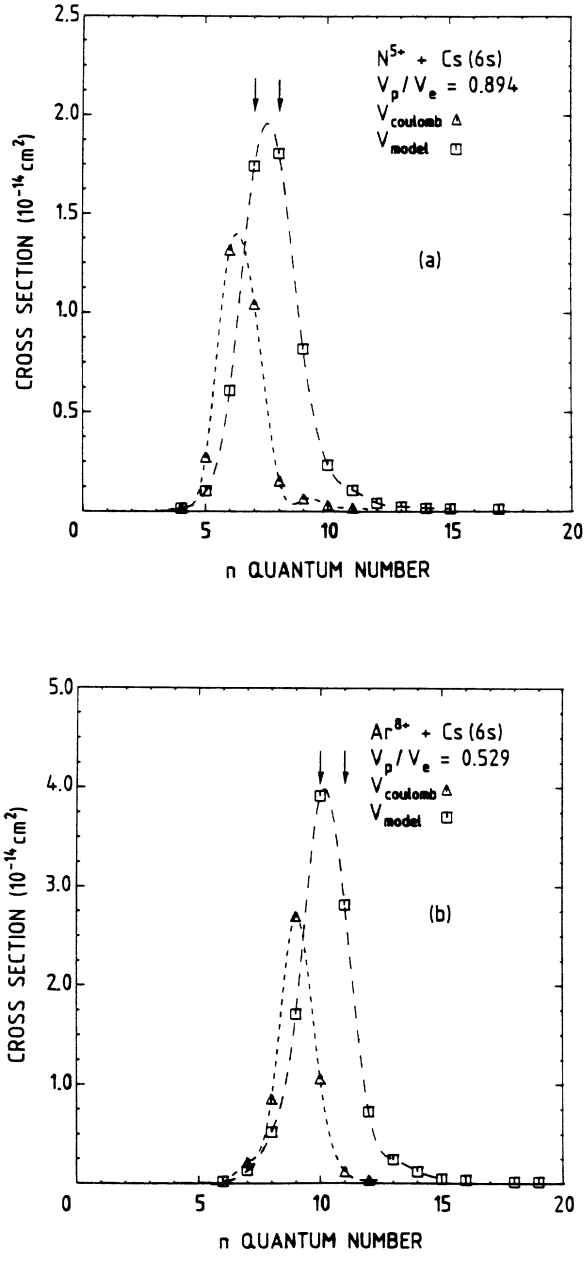

FIG. 7. The electron-capture n distribution for (a) $N^{5+}+Cs(6s)$ collisions at (a) $v_p/v_e=0.894$ and (b) $Ar^{8+}+Cs(6s)$ collisions at $v_p/v_e=0.529$. The open squares and open triangles denote the theoretical results obtained using model potential or pure Coulomb interactions, respectively. The position of the peak is compared to the experimental findings of Martin *et al.* (Ref. 16) (arrows).

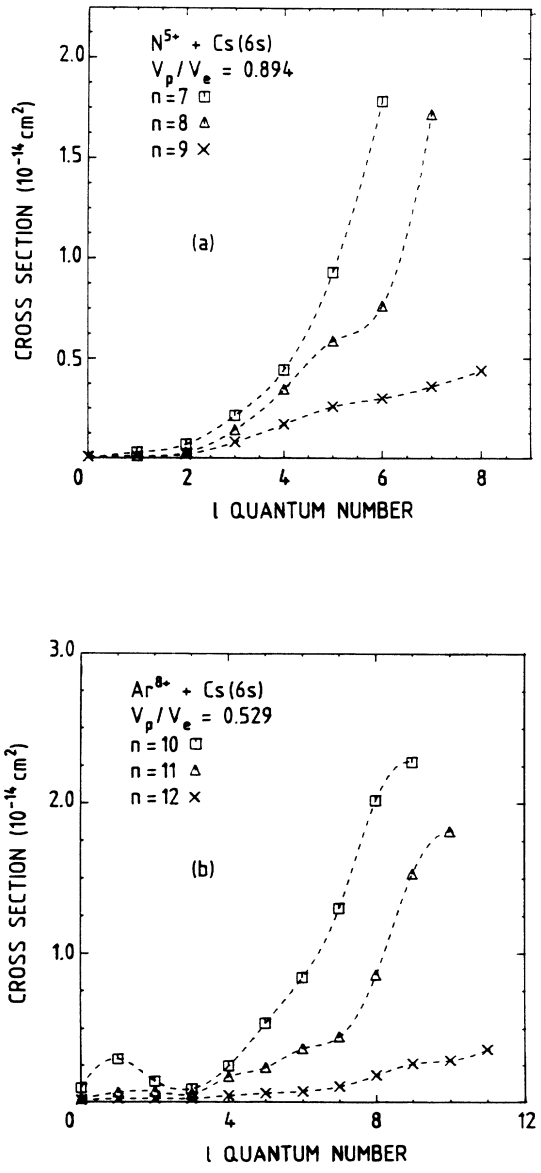

FIG. 8. The calculated n,l distribution [Eq. (10)] for electron capture in (a) $N^{5+}+Cs(6s)$ collisions at $v_p/v_e=0.894$ for $n=7,8,9$ and (b) $Ar^{8+}+Cs(6s)$ collisions at $v_p/v_e=0.529$ for $n=10,11,12$.

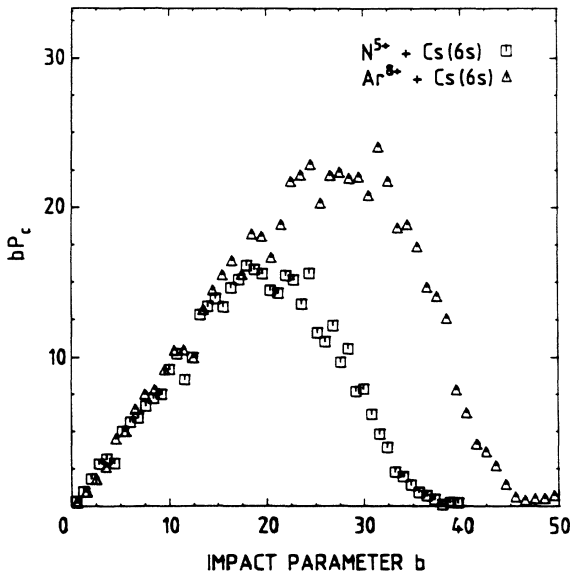

FIG. 9. The calculated probability of electron-capture times the impact parameter in $N^{5+}+Cs(6s)$ collisions at $v_p/v_e=0.894$ (open squares) and in $Ar^{8+}+Cs(6s)$ collisions at $v_p/v_e=0.529$ (open triangles).

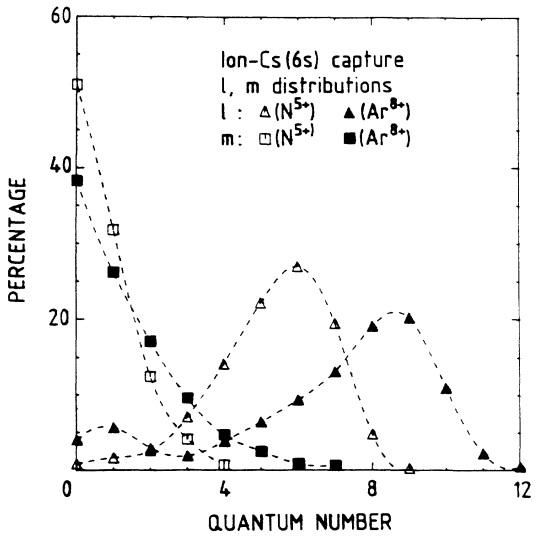

FIG. 11. The calculated percentages of final m and l values for electron capture in $N^{5+}+Cs(6s)$ collisions at $v_p/v_e=0.894$ and $Ar^{8+}+Cs(6s)$ collisions at $v_p/v_e=0.529$.

IV. CONCLUSIONS

Using the three-body CTMC method and a large number of trajectories, we have calculated total and state-selective electron-capture cross sections for $Na^{+}+Na(28d)$ and N^{5+}, $Ar^{8+}+Cs(6s)$ collisions in the intermediate impact velocity range (i.e., $0.5 \lesssim v_p/v_e \lesssim 1.7$). Pure Coulomb and realistic model potential interactions have been employed to simulate the e^{-}-core interactions.

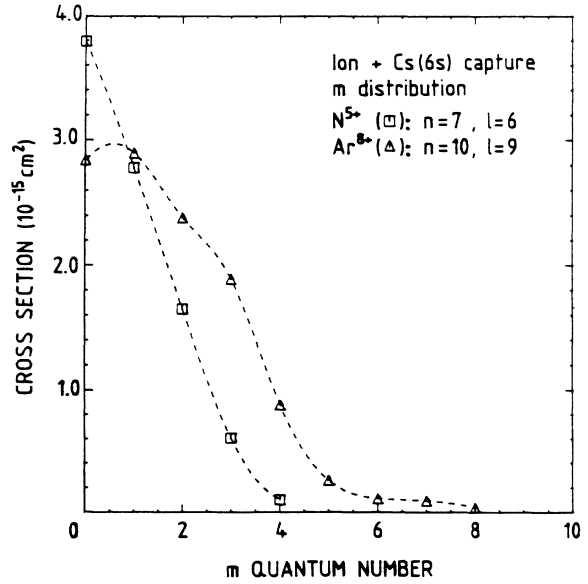

FIG. 10. The calculated n,l,m distribution for electron capture in $N^{5+}+Cs(6s)$ collisions at $v_p/v_e=0.894$ for $n=7$, $l=6$ and $Ar^{8+}+Cs(6s)$ collisions at $v_p/v_e=0.529$ for $n=10$, $l=9$.

We have shown the importance of electron capture into states with large l values. In particular, for N^{5+}, $Ar^{8+}+Cs(6s)$ collisions, we have found that nearly circular states are predominantly populated near the maximum of the final n-level distributions.

More interestingly, we have found that the final m distributions are peaked around $m\simeq 0$ but, also, that they are wider than what is commonly assumed in the literature. In particular, for $Na^{+}+Na(28d)$ collisions we have shown that the contribution of final states with $m\gtrsim 2$ to the total capture cross section near the maximum of the n distribution is greater than 60% for both values of v_p/v_e considered here. In this light, we conclude that diabatic processes should not be neglected in the experimental analysis of the final n distributions by means of the electric-field-ionization technique which is often used when the electron is captured to high Rydberg states. Thus, the present results may be very useful in the analysis of previous experimental data which assumed a pure adiabatic field-ionization process.[12]

For the N^{5+},$Ar^{8+}+Cs(6s)$ collision systems, our results have been found to be in good agreement with recent unambiguous spectroscopic measurements of the most predominantly populated n values. Furthermore, this agreement is obtained only when a realistic model potential (instead of a pure Coulomb potential) is used to describe the e^{-}-Cs^{+} interaction. It is also worthwhile to point out that this agreement is obtained for $v_p/v_e<1$. Nevertheless, an experimental determination of absolute

cross sections near the maximum of the n-level distribution is still needed to assess the accuracy of our calculated cross sections.

Finally, we have shown that the validity range of the CTMC method for the electron-capture process may be extended to $v_p/v_e < 1$ when multiply charged ions are concerned or, more generally, when highly excited states of the projectile are populated.

ACKNOWLEDGMENTS

We would like to acknowledge Dr. A. Pesnelle for stimulating discussions. Also, we are very grateful to Mrs. Nicole Auby for her assistance on the vectorization of the computing codes. This work was partially supported by the Office of Fusion Energy, U. S. Department of Energy.

[1]R. E. Olson, J. Phys. B **13**, 843 (1980).

[2]A. P. Hickman, R. E. Olson, and J. Pascale, *Rydberg States of Atoms and Molecules*, edited by R. F. Stebbings and F. B. Dunning (Cambridge University Press, New York, 1983).

[3]S. Martin, A. Salmoun, Y. Ouardane, M. Druetta, J. Désesquelles, and A. Denis, Phys. Rev. Lett. **62**, 2112 (1989).

[4]D. Banks, R. S. Barnes, and J. Wilson, J. Phys. B **9**, L141 (1976).

[5]R. C. Becker and A. D. MacKellar, J. Phys. B **17**, 3923 (1984).

[6]R. Abrines and I. C. Percival, Proc. Phys. Soc. **88**, 861 (1966).

[7]G. Peach, S. L. Willis, and M. R. C. McDowell, J. Phys. B **18**, 3921 (1985).

[8]S. L. Willis, G. Peach, M. R. C. McDowell, and S. Bararji, J. Phys. B **18**, 3939 (1985).

[9]C. O. Reinhold and C. A. Falcón, Phys. Rev. A **33**, 3859 (1986).

[10]K. B. MacAdam and R. G. Rolfes, J. Phys. B **15**, L243 (1982).

[11]K. B. MacAdam and R. G. Rolfes, J. Phys. B **16**, 3251 (1983).

[12]R. G. Rolfes and K. B. MacAdam, J. Phys. B **15**, 4591 (1982).

[13]A. D. MacKellar and R. L. Becker, *Abstracts of Contributed Papers, Proceedings of the 13th International Conference on the Physics of Electronic and Atomic Collisions, Berlin, 1983*, edited by J. Eichler, W. Fritsch, I. V. Hertel, N. Stolterfoht, and U. Wille (Springer, Berlin, 1983), p. 660.

[14]K. B. MacAdam, L. G. Gray and R. G. Rolfes, *Abstracts of Contributed Papers, Proceedings of the 16th International Conference on the Physics of Electronic and Atomic Collisions, New York, 1989*, edited by A. Dalgarno, R. S. Freund, M. S. Lubell, and T. B. Lucatorto (Elsevier, New York, 1989), p. 728.

[15]K. B. MacAdam (private communication); K. B. MacAdam, L. G. Gray, and R. G. Rolfes, Bull. Am. Phys. Soc. **35**, 1167 (1990).

[16]S. Martin, A. Salmoun, G. Do Cao, T. Bouchama, J. Andrä, and M. Druetta, J. Phys. (Paris) Colloq. **50**, Cl-357 (1989).

[17]J. Pascale, Phys. Rev. A **28**, 632 (1983).

[18]K. B. MacAdam, R. G. Rolfes, and D. A. Crosby, Phys. Rev. A **24**, 1286 (1981).